Continuous Process of the Vacuum Ultraviolet- (VUV-) Photochemical Oxidation of Thiophene in the Gas Phase

Haingo L. Andriampanarivo[1)a)], Martin Köhler[1)b)], Juan López Gejo[1)c)], Thomas Betzwieser[1)d)], Benny C.Y. Poon[2)], Po Lock Yue[2)], Solofonirina D. Ravelomanantsoa[3)], André M. Braun[1)e)]*

[1)] Lehrstuhl für Umweltmesstechnik, Universität Karlsruhe, 76128 Karlsruhe, Germany

[2)] Department of Chemical Engineering, Hong Kong University of Science and Technology (HKUST), Kowloon, Hong Kong, China

[3)] Department of Physics, University of Antananarivo, Antananarivo 101, Madagascar

*) Andre.Braun@kit.edu

Present addresses:

[a)] Institut National des Sciences et Techniques Nucléaires de Madagascar, Antananarivo 101, Madagascar

[b)] Lurgi GmbH, 60439 Frankfurt, Germany

[c)] Business & Technology Incubation Center, SICPA SA, 1008 Prilly, Switzerland

[d)] AREVA GmbH, Reactors & Services, 91058 Erlangen, Germany

[e)] Engler-Bunte-Institut, Karlsruhe Institute of Technology, 76131 Karlsruhe, Germany

Abstract

Thiophene was taken as a model compound for investigations on the efficiency of a continuous process of the vacuum-ultraviolet- (VUV-) photochemically initiated oxidation and mineralization of sulfur containing organic compounds in the gas phase. In the presence of molecular oxygen, atomic oxygen and ozone were photochemically generated and are assumed to initiate or participate in the (thermal) oxidation network. Addition of water vapor for an additional initiation of the oxidation by hydroxyl radicals

did not accelerate the process. For comparison, thiophene was exposed to ozone and oxidized under otherwise the same experimental conditions, but complete mineralization was only found in the photochemical process and for relatively small concentrations of the substrate. The result may be explained by low rates of secondary thermal reactions of a number of identified intermediate products. Combining already published results and mechanistic hypotheses with the results of the present work, pathways of oxidative degradation are proposed. The photolysis of thiophene in molecular nitrogen confirmed earlier findings.

1. Introduction

The continuously increasing emission of hazardous volatile organic (VOC's) and inorganic compounds in industrial and urban areas calls for restrictive measures but also for the development of new methods of air purification that could be installed in a decentralized manner at the sources of pollution as well as in spaces to be particularly protected.

Both, TiO_2-photocatalyzed and vacuum-ultraviolet- (VUV-) photochemical oxidation of gaseous pollutants exhibit rather high efficiencies, and continuous processes may be developed and installed at different scales. They are attractive alternatives to conventional methods of air purification, like adsorption and subsequent incineration or wet-chemical treatment of pollutant-loaded adsorbants [*e.g.* 1]. Both processes exhibit specific advantages and constraints that merit to be investigated in detail [*e.g.* 2, 3], and the combination of the two methods of air treatment might have a very high application potential for the abiotic treatment of polluted air [4 - 10].

After exploring the VUV-photochemical oxidation of hydrocarbons, halogen as well as N- and O-containing organic substrates chosen as model pollutants [11 - 16], this work focuses on thiophene (**TP**, Scheme 1) as a S-containing organic compound. Among the different volatile organic compounds (VOCs) present in industrial and urban emissions, **TP** is one of the most important because of its presence in fossil fuels [*e.g.* 17]. As a S-organic compound, it is an important contributor to acid rain due to its oxidative

degradation in the troposphere. Its toxicology and effects on some metabolic processes were demonstrated [18]. At the same time, **TP** is widely used as a building block in agrochemicals and pharmaceuticals, dyes and resins [19].

The VUV-photochemical oxidation of gaseous **TP** in the presence of O_2 is at least in part a VUV-photochemically initiated oxidation consisting essentially of the thermal oxidation of the substrate initiated by reactive oxygen species. Depending on the experimental conditions chosen, four major reaction pathways may be differentiated: (i) initiation by atomic oxygen (O) that is generated by the VUV-photolysis of molecular oxygen (O_2) as a component of the bulk gas phase (reactions (1) [27], (ii) oxidation by ozone (O_3) produced by reaction (2) [21, 22], (iii) initiation by hydroxyl radicals ($HO^{\cdot}$) [23 - 26] formed by the VUV-photolysis of water (H_2O) vapor contained in the gas phase (reaction (9)), and (iv) photolysis of **TP** and subsequent trapping of radical intermediates by O_2.

Earlier work demonstrated the high efficiency of oxidative pollutant degradation as a result of the combination of the two VUV-photochemical processes [14]. In particular, alkanes, alkenes, arenes and oxygen containing organic compounds could be mineralized in continuously driven processes. Depending on the concentration of **TP** in the gas phase, electronic excitation of the substrate might be possible, and investigations on the photochemical reactivity were published [27 -30] and related reactions taking place in the troposphere [e.g. 31].

1.1. VUV-photochemical initiation of oxidative degradation

Upon excitation at wavelengths $\lambda_{exc} < 200$ nm, O_2 homolyzes to atomic oxygen (O, reaction (1)) [20], the latter adding to O_2 to produce O_3, (reaction (2)) or reacting with an organic molecule by H-abstraction (reaction (3)) or by insertion into a σ-bond (e.g. C-H (reaction (4)).

$$O_2 + h\nu \longrightarrow 2\,O \tag{1}$$

$$O + O_2 \longrightarrow O_3 \tag{2}$$

$$O + RH \longrightarrow HO^{\cdot} + R^{\cdot} \tag{3}$$

$$O + RH \longrightarrow ROH \tag{4}$$

Generated efficiently by reactions (1) and (2) [32], O_3 is not photolyzed by VUV-radiation emitted by a Xe-excimer lamp (λ_{exc}: 172 nm). The oxidant is an electrophile and adds in the case of the present study either to C=C-bonds to yield ozonides that subsequently fragment into carbonyl and/or carboxyl compounds depending on substrate structure and experimental conditions [33] or to the S-function (s. § 1.4.).

For the gas phase reaction of O with **TP**, a rate constant $k_{O/TP} = 1.2 \times 10^{-11}$ cm^3 molecule^{-1} s^{-1} was reported [34, 35], and, based on hypotheses published in the latter reference, it may be assumed that O might insert into the α-C-H bond (reaction (5), Scheme 1) or add to one of the free electron pairs of S (reaction (6), Scheme 1). C-H bond insertion and addition to a C=C bond (reaction (7), Scheme 1) [36] with subsequent proton shift would lead to the same 3- and 5-thiolen-2-ones (3H-2-thiopheneone (**2**) and 5H-2-thiopheneone (**3**), respectively, Scheme 1). As far as addition to the S-function is concerned, the inverse reaction of generating O by electronic excitation was reported for thiophene-1-oxide (**4**, reaction (8), Scheme 1), and some of its derivatives [36 - 38].
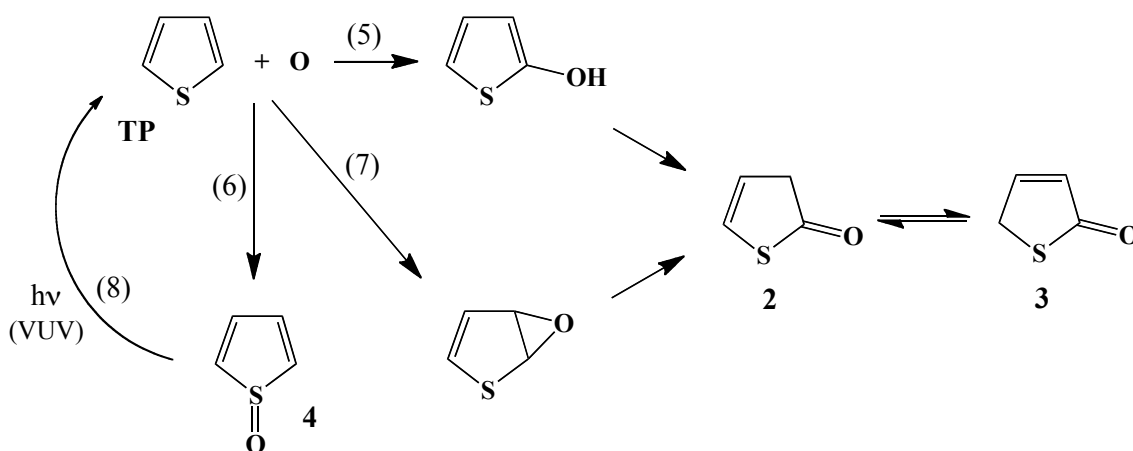
Scheme 1. Reactions of atomic oxygen with thiophene (**TP**, s. references in the text).

H_2O in condensed and gaseous phases is known to homolyze into atomic hydrogen (H$^{\bullet}$)

and HO$^{\bullet}$ upon excitation at $\lambda_{exc} <$ 190 nm (reaction (9)) [39]. While the first is efficiently trapped by O_2 to yield hydroperoxyl radicals (HO$_2^{\bullet}$, reaction (10)), the latter reacts with organic substrates by H-abstraction (reaction (11)) or by addition to π-systems (*e.g.* aromatic moieties, reaction (12)) [40].

$$H_2O + h\nu \longrightarrow H^{\bullet} + HO^{\bullet} \tag{9}$$

$$H^{\bullet} + O_2 \longrightarrow HO_2^{\bullet} \tag{10}$$

$$HO^{\bullet} + RH \longrightarrow H_2O + R^{\bullet} \tag{11}$$

$$\tag{12}$$

In the gas phase, the rate constant of the addition of HO$^{\bullet}$ to **TP** ($k_{HO*/TP}$) was determined to be between 1.1 x 10^{-11} and 9.5 x 10^{-12} cm^3 molecule^{-1} s^{-1} [22a, 26]. Subsequent reaction pathways were, however, so far not investigated, and the results of the experiments made in the presence of a defined concentration of H_2O will be discussed with reference to data obtained in condensed aqueous phase [41].

1.2. VUV-photolysis

Depending on the experimental conditions (bulk gas, wavelength(s) of irradiation, concentrations of VOCs and gaseous H_2O), the VUV-photolysis of the VOCs might compete with the VUV-photochemically initiated oxidation processes. Within the spectral region of interest, the absorption spectrum of gaseous **TP** shows two absorption bands at approx. 225 and 176 nm (Figure 1)) being assigned to π,π^* transitions [42, 43]. The absorption cross section at 172 nm ($\sigma_{TP,172}$) is calculated from the spectrum shown in Figure 1 to be 6.3 x 10^{-17} cm^2. Excitation at 172 nm, corresponding to an energy of 7.2 eV photon^{-1}, cannot ionize **TP** whose lowest ionization potential is 8.9 eV [44].
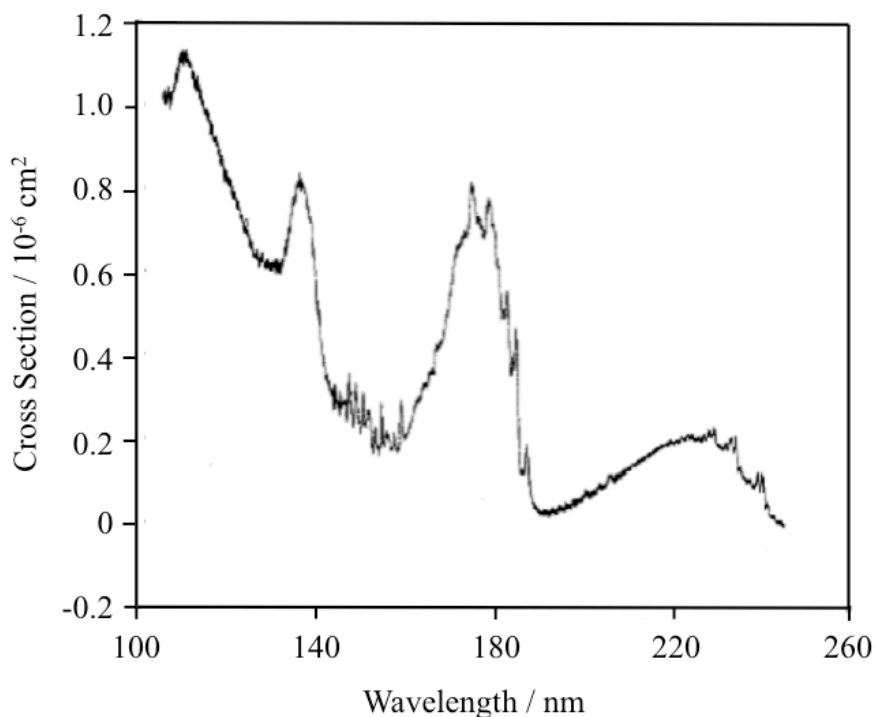
Figure 1. VUV- and UVC-spectrum of gaseous thiophene (**TP**), adapted from [45].

The lowest energy absorption band being located in the UV-C spectral domain and assuming that Kasha's rule is valid in the case of **TP**, the results of the UV-C photolysis of gaseous **TP** might serve as a lead for the interpretation of the results presented in this paper. In the absence of O_2, irradiation in the spectral domain between 214 and 229 nm led to C-S-bond homolysis as the major reaction path (reaction (13), Scheme 2) generating the corresponding 1-thiapenta-2,4-diene-1,5-diyl biradical (**5**) from which 1-buten-3-yne (**6**), atomic sulfur, ethyne (**8**), thioethenone (**9**), propyne (**14**), carbon monosulfide and 1-thia-2-propene-1,3-diyl (**7**), cyclobutadienyl (**10**), sulfanyl (**11**), propargyl (**12**), thioformyl (**13** radicals (reactions (13a - e)), Scheme 2) as well as non-identified polymers were produced [27]. Similar experiments in the presence of O_2 yielded O-containing organic products that were not identified, but the production of carbon dioxide (CO_2), carbon monoxide (CO) and carbonyl sulfide (OCS) confirmed the oxidation of primary intermediates. Although SO_2 was found, its qualitative analysis alone was considered insufficient to conclude on the priority of S-oxidation within the

network of a photochemically initiated oxidative degradation of **TP** [27]. Experiments with IR multiphoton excitation [46] and by VUV-laser photolysis at 193 nm [28] confirmed the earlier results of Wiebe and Heicklen [27]. An observed transient with absorption between 377 to 417 nm was tentatively assigned to **10** (reaction (13c), Scheme 2) [47]. The reaction network (reactions (13a - e) in Scheme 2 is taken from a detailed analysis of the products upon photo-fragment translational spectroscopy (λ_{exc}: 193 nm) [48]. All reactions are subsequent to the formation of **5** (reaction (13), formation of sulfur (reaction (13a)) and elimination of **8** (reaction (13b)) being most favored, whereas the homolysis of hydrogen was excluded [48, 49].

In O_2-containing gas phases, intermediate C- and S-centered radicals are trapped yielding the corresponding peroxyl radicals (reaction (14), s. § 1.3.)
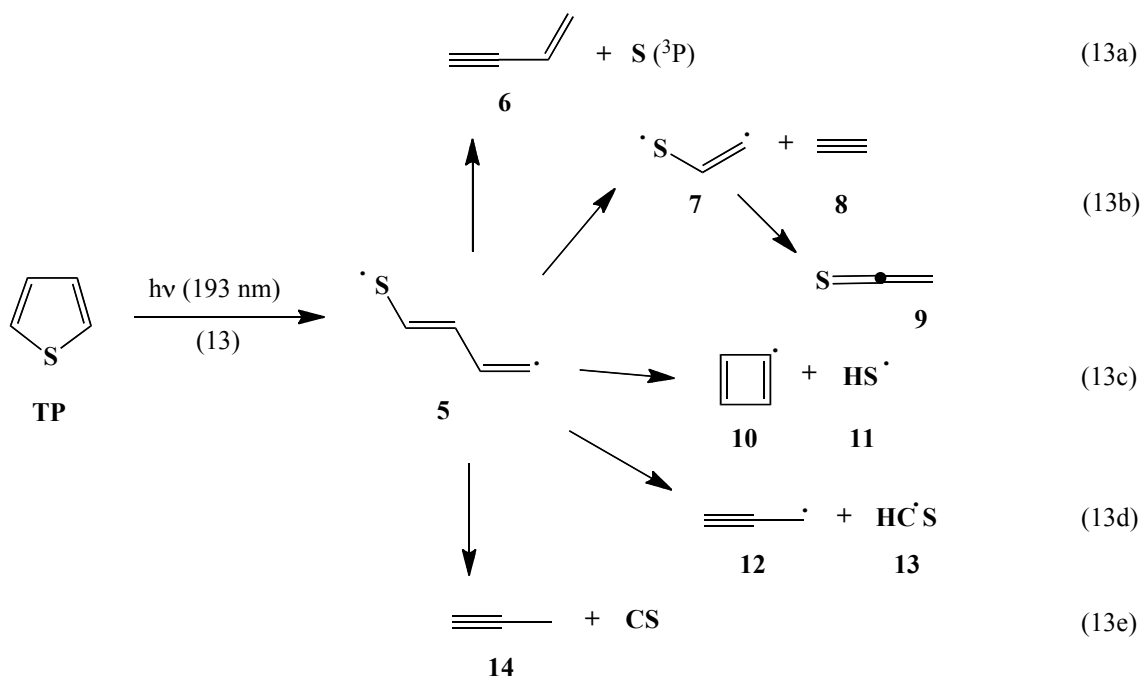
Scheme 2. Products of the primary reaction (13) upon electronic excitation of thiophene (**TP**, λ_{exc}: 193 nm) [48].

1.3. VUV-photochemical oxidation and mineralization

The C-and S-centered radicals formed in reactions (3), (11), (13) and (13b-d) may react with O_2 to form peroxyl radicals (reaction (14)) which are considered to be the key

intermediates in subsequent thermal oxidation reactions leading ultimately to complete oxidation of the organic carbon, *i.e.* mineralization [40].

$$R^{\cdot} + O_2 \longrightarrow RO_2^{\cdot} \qquad (14)$$

The present work focuses on the VUV-photochemically initiated oxidation of gaseous TP, and more specifically on the efficiencies of continuous oxidative degradation processes depending on the initiating species. The intermediate products and the overall rates of the oxidation are compared with those of the oxidation by ozonolysis.

1.4. Ozonolysis of thiophene (TP)

The rate constant of the reaction of O_3 with **TP** ($k_{O_3/TP}$) was determined to be 6 x 10^{-20} cm^3 molecule^{-1} s^{-1} [22]. Ozonolysis was reported to yield almost quantitative desulfurization (analysis of sulfur dioxide (SO_2)) and rather high quantities of CO_2. Consequently, a major reaction channel producing intermediate butadiene and/or butene may be assumed, both intermediates being subsequently either mineralized, or polymerized and thus sequestered from gas analysis [21].

2. Experimental Part

2.1. Photolysis equipment

Scheme 3 shows a complete view of the experimental set-up consisting of three main parts: (i) the photochemical reactor, (ii) the flow control and mixing system and (iii) the gas analyses.
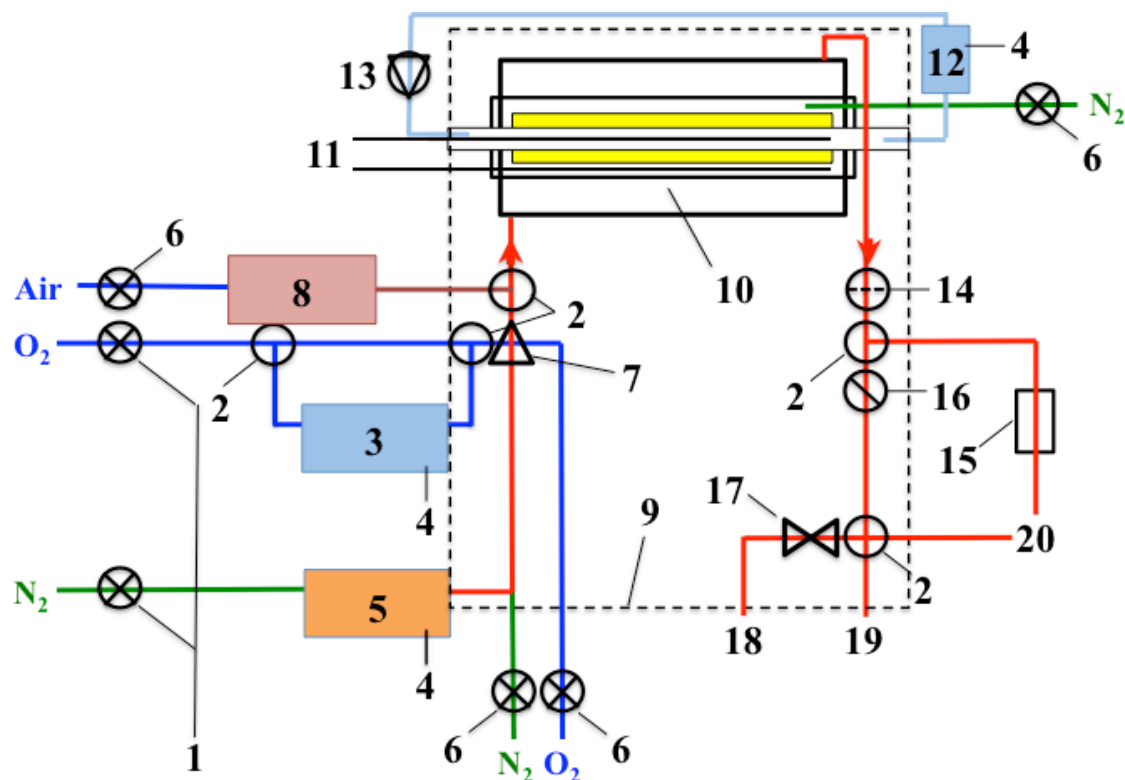
Scheme 3. Scheme of experimental set-up for a continuous VUV-photochemical oxidation of thiophene (**TP**) in the gas phase. 1: Digital flow controls, 2: 3-way valves, 3: H_2O-saturation, 4: Thermoregulation, 5: Controlled introduction of thiophene, 6: manual flow controls, 7: Gas mixing, 8: Ozonizer, 9: Thermoregulated space, 10: Photochemical reactor, 11: Power supply for Xe_2-excimer radiation source (200 W), 12: Reservoir and heat exchanger for closed cooling circuit with de-ionized water, 13: Pump, 14: Filter, 15: UV-photometer, 16: Manometer, 17: Reducing valve, 18: GC-analysis with automatic injection, 19: exit for off-line analyses, 20: hood.

2.1.1. *Photochemical reactor*

The photochemical reactor consisted of an outer tube made of Duran® with an inner diameter of 10.5 cm. The co-axially mounted water-cooled Xe_2-excimer radiation source (Lichttechnisches Institut, Universität Karlsruhe, Germany) was enwrapped with a potential bearing net-electrode (steel) and inserted into a Suprasil® protection tube with an outer diameter of 5.8 cm leaving an optical path length ($r_{ext} - r_{int}$) of approx. 2.3 cm.

The grounded electrode was placed into the inner tube of the radiation source through which the cooling water (deionized) was introduced. The radiation source was operated with an ENI power supply (5000 V, 180 kHz) with an electrical power of 200 W. The volume containing the potential bearing electrode was continuously purged with N_2 during irradiation experiments. Condensation of the gaseous components of the reaction system was avoided by maintaining an overall reactor temperature of 80 °C. Gases were introduced into and taken from the reactor by lateral connections placed toward the ends of the outer reactor tube. The length of the reactor was 19 cm to yield a reactor volume of approx. 1150 cm^3.

2.1.2. *Flow-control and gas-mixing system*

The flow-control and gas-mixing system allowed the monitoring the flows of different gas streams to be irradiated and to vary their content of **TP**, O_2 and H_2O using N_2 as the bulk gas.

Experiments in the absence of H_2O were carried out with a total gas flow of 500 cm^3 min^{-1} that was composed of three gas streams:

(a) 245 cm^3 min^{-1} of O_2 (99,995%, Messer Griesheim)

(b) 225 cm^3 min^{-1} of N_2 (99,999%, Messer Griesheim)

(c) 30 cm^3 min^{-1} of N_2 (99,999%, Messer Griesheim) containing a defined concentration of **TP** (c_{TP}).

Experiments in the presence of H_2O were carried out with a total gas flow of 500 cm^3 min^{-1} that was composed of three gas streams:

(a') 120 cm^3 min^{-1} of H_2O-saturated O_2, prepared by passing O_2 through a gas-washing bottle containing tri-distilled water. The bottle was immersed in a water bath maintained at 80°C.

(b') 225 cm^3 min^{-1} of N_2 and 125 cm^3 min^{-1} of O_2

(c') 30 cm^3 min^{-1} of N_2 containing a defined concentration of **TP** (c_{TP}).

Experiments in N_2 were carried out with a total gas flow of 500 cm^3 min^{-1} that was composed of two gas streams:

(b'') 470 cm^3 min^{-1} of N_2

(c'') 30 cm^3 min^{-1} of N$_2$ containing a defined concentration of **TP** (c_{TP})-

The partial gas-flows were continuously checked by flow controllers. With a reactor volume of 1150 cm^3, the residence time for all experiments was 2.3 min.

A defined concentration of **TP** was introduced into the stream of the carrier gas by means of a diffusion cell [50]. It consisted of a thermoregulated reservoir containing liquid **TP** in equilibrium with the gas phase. Gaseous **TP** diffused through a calibrated glass tube into a mixing sphere, from where it was carried by the stream of N$_2$ toward the mixing zone to prepare the reaction system. The amount of **TP** in the gas phase is a function of the temperature of the bath, the dimensions of the calibrated glass tube (diameter and length) and the flow of the carrier gas (N$_2$). The concentration (c_{TP}) introduced by streams (c), (c') or (c'') may be calculated from the mass of the substrate mixing with the carrier gas per unit time (Q_{TP}, s. Electronic supplementary information (ESI)). The calculated concentrations and the stability of c_{TP} introduced into the continuously irradiated reaction system were independently checked by gas chromatography (Figures ESI 1 and ESI 2). Calibration was made with standard solutions of **TP** in *n*-hexane using concentrations within the working range (s. § 2.1.4).

2.1.3. Evaluation of photolysis conditions
s. Electronic supplementary information (ESI).

2.1.4. Ozonolysis
Ozone (O$_3$) was produced from synthetic air (Messer-Griesheim) by an ozonizer (Labor-Ozonizer 301, Sander, Uetze-Eltze, Germany) and fed with N$_2$ into the dark photochemical reactor. Fluxes of N$_2$ and O$_2$ during ozonolysis into the reactor were adjusted to the total gas flow of 500 cm^3 min^{-1}. The ozone concentration (c_{O_3}) in the dark photochemical reactor was analyzed at the exit by UV (254/255 nm) absorption measurements (s. [16]) and adjusted to the concentration that was measured during irradiation of oxygen/nitrogen mixtures in the absence of **TP** to 1650±35 ppm (v/v).

2.1.5. Analytical Techniques

The gaseous mixture exiting the reactor (500 cm^3 min^{-1}) was divided into a flow of 20 cm^3 min^{-1} used for on-line analysis of gaseous organic compounds by gas chromatography (GC) and a flow of 480 cm^3 min^{-1} to be used for the off-line analyses by GC/MS and of CO_2 and SO_2 by Fourier Transform Infrared Spectroscopy (FTIR) and ion chromatography (IC).

Gas chromatography (GC) analyses of **TP** were performed with a HP 5896 Series II equipped with a FID detector (Agilent Technologies). Samples were automatically collected via a 6-way valve by a calibrated loop (sampled volume: 0.25 cm^3, 180ºC) and injected (220ºC, Figure ESI 2a). An INNOWAX® column (30 m x 0.32 mm x 0.25 μm) was installed and operated at 30ºC with a He flow of 2.4 cm^3 min^{-1} (split: 1/10). The GC analysis of **TP** was calibrated with standard solutions of **TP** in *n*-hexane, and, within the concentration range used for the photochemical experiments, a linear response was obtained (Figure ESI 3). Each standard solution was analyzed three times, and a reproducibility with the error of < 5% was found. Figure ESI 1 shows a good agreement between the calculated and the experimental values of c_{TP} within the experimental range of 30 ± 10ºC. The stability of c_{TP} exiting the diffusion cell, of the mixing of gas streams (c), (c') and (c'') with the carrier gas streams and of the automatic injection into the GC equipment depended strongly on the pressure stability and represented a major technical problem of the equipment conceived for this work. Satisfactory pressure stability was achieved by maintaining an overall overpressure of 14 mbar. (Figure ESI 2b). Integration of the GC-peaks representing **TP** (Figure ESI 2a) and conversion of the respective areas by means of the calibration curve (Figure ESI 3) yielded c_{TP} (Figure ESI 2b) exiting the reactor.

The GC-analyses of CO_2 were performed with a HP 3365/5890I Series II equipped with a TCD detector (Agilent Technologies). Samples were automatically collected via a 6-way valve by a calibrated loop (sampled volume: 0.25 cm^3, 180ºC) and injected (220ºC). A GS-GasPro column (60 m x 0.32 mm x μm) was installed and used at 50ºC with a He flow of 1.4 cm^3 min^{-1} (split: 1/10). The analyses were calibrated with flow controlled mixtures of 1.51% of CO_2 in N_2 (99,999%,, Messer-Griesheim) and N_2 (99,999%,

Messer-Griesheim) to obtain the same flux conditions as chosen for the irradiation experiments. The resulting linear function between the values of the integrated areas of the chromatographic peaks and the moles of CO_2 contained in the injected samples (Figure ESI 4) allowed the determination of the number of moles of CO_2 produced by the VUV-photochemically initiated oxidative degradation of **TP**.

Gas chromatography/mass spectrometry (GC/MS) analyses for product identification were made with a HP 5973 GC/Selective MS-Detector combination (Agilent Technologies). A VOC$^{®}$ column (60 m x 0.2 mm x 1.1 μm, Agilent Technologies), was used at 30°C with a He flow of 2.4 cm^3 min^{-1}. For identification, mass spectra were compared with those available in the library of the software ChemStation G1701BA, version B.01.00 (Agilent Technologies).

Ion Chromatography was used for the quantitative analysis of SO_2. For this purpose, the exiting gas flow was introduced during a sampling time of 6 min (f_R: 480 cm^3 min^{-1}, sampling volume (V_s): 2880 cm^3) into a gas-sampling bag containing 50 cm^3 of a solution made from 30 cm^3 of (30% v/v) H_2O_2 and 0.1 cm^3 of 0.6 M HCl and diluted to 1 L. The SO_2 is absorbed and oxidized to SO_3 and passes into the solution as SO_4^{-2} to be subsequently analyzed using a HP 1050 Ti-Series liquid chromatograph (Agilent Technologies) equipped with a precolumn AG12A 4 mm (10-32) (Dionex GmbH, Germany), an anionic exchange column AS12 A 4mm (10-32) and a Dionex CD20 conductivity detector. A solution of 2.4 x 10^{-3} M of Na_2CO_3 and 0.3 x 10^{-3} M of $NaHCO_3$ served as eluent with a flow of 0.10 cm^3 min^{-1}. Calibration was made with aqueous solutions of Na_2SO_4 in the range of 2.7 x 10^{-5} to 3.1 x 10^{-4} M.

Fourier Transform Infrared (FTIR) Spectroscopy was also used for the quantitative analysis of CO_2, but experiencing interferences with other triatomic gases like SO_2, H_2O or O_3, the on-line IR-analysis of small values of c_{CO_2} was not viable. For sampling, the exiting gas mixture was led through a cold-trap and a drying tube ($CaCl_2$) before filling the FTIR spectroscopic cell. The cell consisted of a cylindrical glass tube (length: 23 cm, i.d.: 2.5 cm) with two KBr windows and two connections for the gas sampling controlled with valves. Before each analysis, the FTIR spectrometer (Bruker, Equinox 55) equipped with a DTGS (Deuterated Triglycine Sulfate) detector had to be purged

with N_2 for 2 hours to eliminate atmospheric CO_2 that would interfere with the measurement. CO_2 was quantified by measuring the absorption of the double-band between 2200 - 2400 cm^{-1}, after calibration with standard mixtures of CO_2 in N_2 (Messer-Griesheim). A FTIR-spectrum of N_2 served as a blank.

3. Results and Discussion

3.1. Efficiency of the VUV-photochemically initiated oxidative degradation

There are few studies on abiotic photochemical oxidative degradation of both benzothiophene [52] and **TP** [53]. Continuing exploratory work on the use of VUV-photochemical processes for the oxidative degradation of organic materials, the present study evaluates the efficiency of this technique for the oxidative degradation of **TP** as a model compound for the class of S-containing VOCs. The A_{172}-data provided (§2.1.3) show that under the given experimental conditions, three to four parallel pathways of oxidation are to be taken into account:

- absorbing species O_2: initiating oxidation of **TP** by O (reactions (3) and/or (4)) e.g. [20, 34, 35],

- absorbing species O_2: initiating oxidation of **TP** by O_3 [33, 54],

- absorbing species **TP**: oxidation by addition of O_2 to intermediate radicals generated by the photolysis of **TP** (reaction (13)) [27],

- absorbing species H_2O: initiating oxidation of **TP** by $HO^{\bullet}$ (reactions (11) and (12)) [39, 55].

Figure 2 shows a typical series of c_{TP} (ppm (v/v), 1 ppm (v/v) = 1.25 x 10^{-5} mole cm^{-3} (80ºC)) profiles as a function of time of the continuous photochemical process. Approximately one minute after the radiation source was switched-on, **TP** entering into the photochemical reactor could no longer be detected at the exit. The chosen residence time of 2.3 min was more than sufficient for a quantitative oxidation of the substrate (up to *e.g.* 53 ppm (v/v), Figure 2). In fact, quantitative oxidation of **TP** was tested and

established until an initial c_{TP} of 170 ppm (v/v) was reached. When the radiation source was switched off, c_{TP} increased slowly to reach the initial values.
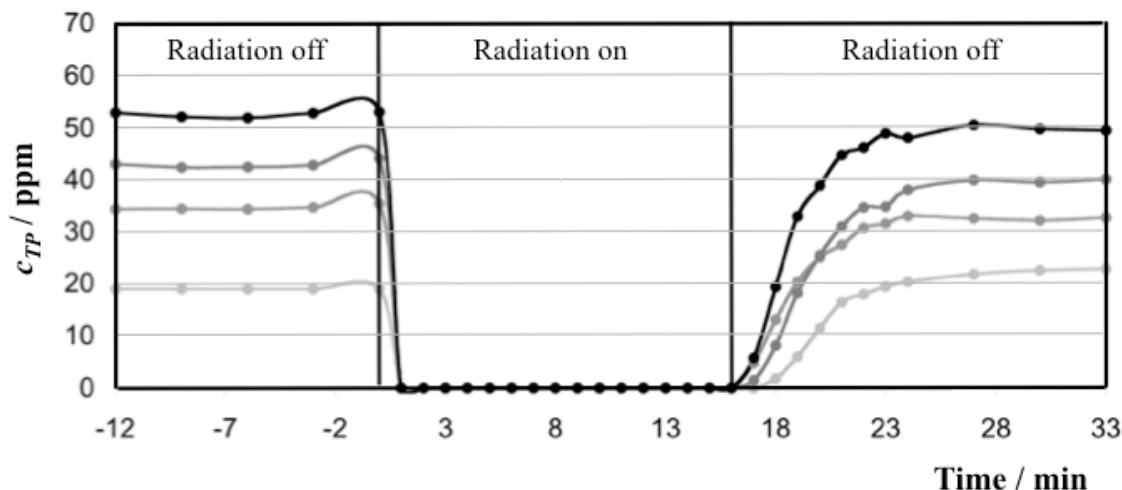
Figure 2. Continuous VUV-photochemically initiated oxidation of gaseous thiophene (**TP**) in the absence of H_2O. Evolution of c_{TP} in function of reaction time for initial c_{TP} ranging from 18 to 53 ppm (v/v). Diffusion cell: f_{N_2} = 30 cm^3 min^{-1}, f_T = 500 cm^3 min^{-1}, residence time: 2.3 min, Xe$_2$-excimer lamp: 200 W.

Quantitative consumption of **TP** does not necessarily mean that the organic substrate is completely mineralized. In order to evaluate the efficiency of the process to mineralize the organic substrate, CO_2-analyses of the gaseous mixtures exiting the reactor were made and allowed the investigation of the evolution of CO_2 in the presence and absence of water vapor. Complete mineralization could not be observed during the time of the experiment (20 min, Figure 3). The results indicate, however, that the consumption of **TP** was less efficient in the presence of H_2O, quantitative oxidation of **TP** being reached after approximately 5 times the process time needed in the absence of gaseous H_2O.
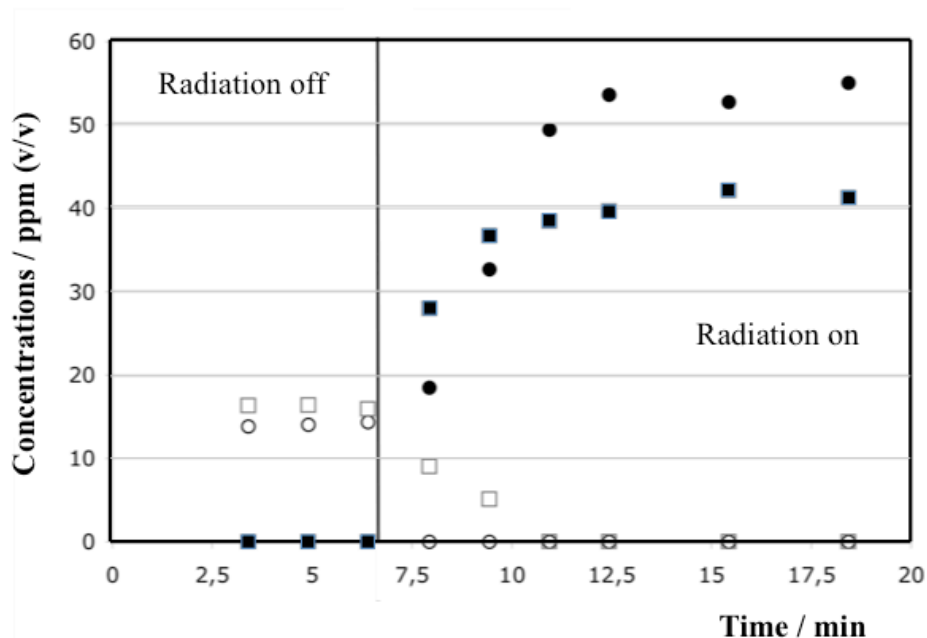
Figure 3. Continuous VUV-photochemically initiated oxidative degradation of gaseous thiophene (**TP**). Evolution of c_{TP} and c_{CO_2} in the presence and absence of H_2O. c_{TP} : 14 ppm, diffusion cell: f_{N_2} = 30 cm^3 min^{-1}, f_T = 500 cm^3 min^{-1}, residence time: 2.3 min, Xe_2-excimer lamp: 200 W. $\bigcirc$: c_{TP} during VUV-photolysis in the presence of O_2 and in the absence of H_2O; $\square$: c_{TP} during VUV-photolysis in the presence of O_2 and H_2O; $\bullet$: c_{CO_2} during VUV-photolysis in the presence of O_2 and in the absence of H_2O; $\blacksquare$: c_{CO_2} during VUV-photolysis in the presence of O_2 and H_2O.

Right after the introduction of the substrate into the reactor, mineralization in the presence of H_2O seemed most efficient, but the process slowed down considerably after the first 5 minutes, and the rate of mineralization was found generally higher in the absence of H_2O (Figure 4). Complete mineralization could only be observed in the absence of H_2O until an initial c_{TP} $\leq$ 22 ppm. With increasing c_{TP}, the rate of mineralization dropped to approximately 20% for c_{TP} = 90 ppm. For values of c_{TP} < 50 ppm, the lower rates of **TP** oxidation and mineralization obtained in the absence H_2O might be surprising, because the A_{172} -data favor reaction (9) in comparison to reactions

(1) and (13), and the rate constant of reaction (15), $k_{O/H_2O} = 2.3 \times 10^{-10}$ cm^3 molecule^{-1} s^{-1} [51], is similar to those expected for reactions (14), *e.g.* [1.5 x 10^{-10} cm^3 molecule^{-1} s^{-1} [3] but higher than that of O with **TP** ($k_{O/TP} = 1.2 \times 10^{-11}$ cm^3 molecule^{-1} s^{-1} [34, 35]).

However, the high value of $A_{H_2O,172}$ confines the primary radicals H$^{\cdot}$ and HO$^{\cdot}$ (reaction (9)) to an extremely small irradiated volume [56] within which rapid depletion of the concentrations of O$_2$ and **TP** (reactions (10) and (14), respectively) occurs, while a more important fraction of the gas mixture passes the reactor unreacted. Given the constant rate of H$^{\cdot}$ and HO$^{\cdot}$ generation [55], the local concentrations of O$_2$ and **TP** depend on the rate of their diffusion into the irradiated volume. It may therefore be assumed that the rate of consumption of **TP** readjusted within a few minutes of process time to these conditions, and the less efficient mineralization would be due to local O$_2$-deficiency.

$$O + H_2O \longrightarrow 2\ HO^{\cdot} \tag{15}$$
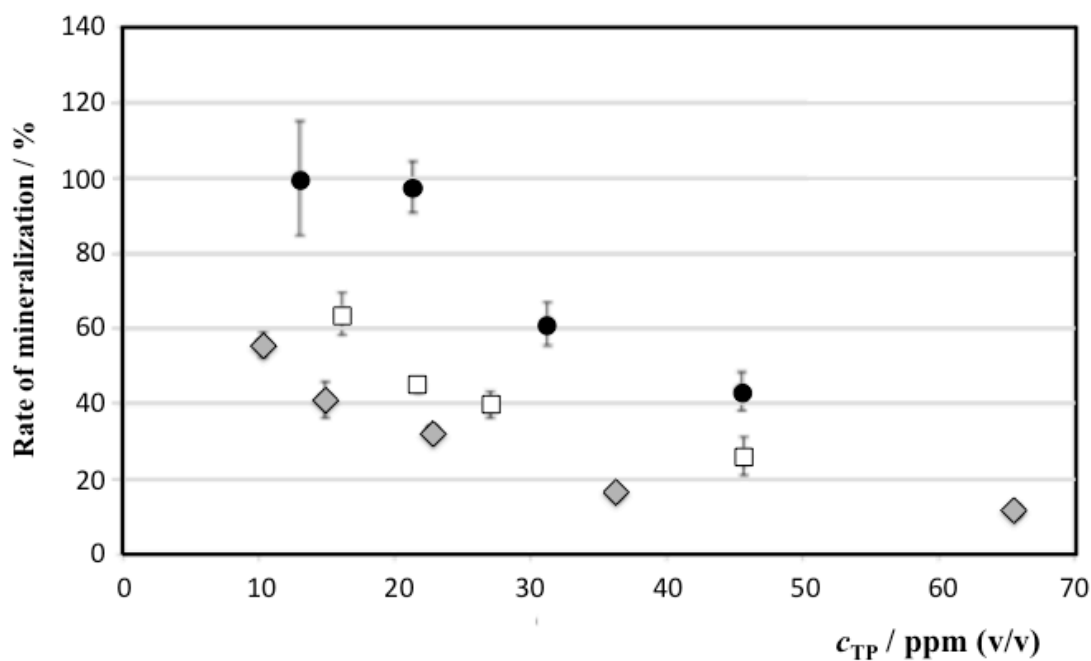
Figure 4. Oxidative degradation of thiophene (**TP**). Efficiency of mineralization (maximum c_{CO_2} analyzed, in % of the stoichiometric initial c_{TP}) depending on the mode of initiation (VUV-photochemical initiation in the presence and absence of water vapor or ozonolysis). Diffusion cell: f_{N_2} = 30 cm^3 min^{-1}, f_T = 500 cm^3 min^{-1}, residence time: 2.3 min, Xe$_2$-excimer lamp: 200 W, c_{O_3}: 1650±35 ppm (v/v). ●: VUV-photolysis in the presence of O$_2$ and in the absence of H$_2$O; □: VUV-photolysis in the presence of O$_2$ and H$_2$O; ◈: Ozonolysis.

All three oxidants (O, O$_3$ and HO$^•$) also react with the S-function of **TP** [33 - 35, 54, 57] to form the corresponding sulfoxide (thiophene 1-oxide (**15**)) and sulfone (thiophene 1,1-dioxide (**16**), Scheme 4), the latter being assumed to eliminate SO$_2$ in the course of an oxidative degradation. SO$_2$-analyses exhibit decreasing concentrations of SO$_2$ (c_{SO_2}) for initial c_{TP} increasing from 39 to 235 ppm (v/v) (Table 1). For all c_{TP} investigated, values of c_{SO_2} were found higher than those of the corresponding c_{CO_2}. The result is, however, no indication that formation of **16** and subsequent SO$_2$-elimination is the predominant pathway of the oxidative degradation of **TP**. In fact, Table 1 indicates that, even in the case of a quantitative oxidation of **TP**, relatively important fractions of intermediate oxidation products remain in the exit gas, some of them still containing a S-function.

Table 1. Maximum c_{SO_2} (ppm (v/v and % of the stoichiometric initial c_{TP}) found in gas mixtures exiting the photochemical reactor during the VUV-photochemical oxidative degradation of thiophene (**TP**) in the absence of H$_2$O. Comparison with stoichiometrically corrected results of corresponding CO$_2$-analyses.

Initial c_{TP} [ppm]	c_{SO_2} analyzed [ppm]	% SO$_2$ ±10%	% CO$_2$ [a)] ±10%
20			100
30			60

39	30	77	
46			43
50	35	70	
82			30
96	56	58	
149	69	46	
235	103	44	

[a] Values taken from Figure 4.

3.2. Intermediate products of the reaction pathways to the mineralization of thiophene.

The kinetics of oxidation and mineralization of gaseous **TP** and the analyses of CO_2 and SO_2 yielded information on the effect of the addition of H_2O on the importance of the oxidation of the S-function and the mineralization of the substrate. In order to obtain more insight into the different pathways of oxidation depending on the mode of excitation and/or initiation, an investigation on the intermediate products of the oxidative degradation might be helpful. However, all three initiators (O, O_3 and $HO^•$) being electrophiles, the primary pathways of oxidation might lead to identical primary products of oxidation.

With O_2 present in the initial gas mixture, VUV-radiation generates O (reaction (1)) as one of the agents initiating the oxidation network. Furthermore, O_3 is produced (reaction (2)) and known to react with the substrate. The rate constant of the reaction of O_3 with **TP** ($k_{O_3/TP}$ = 6 x 10^{-20} cm^3 molecule^{-1} s^{-1} [22]) is approximately 10^8 times smaller than the corresponding rate constant of the reaction of O ($k_{O/TP}$ = 1.2 x 10^{-11} cm^3 molecule^{-1} s^{-1} [34, 35]). Nevertheless, oxidation and mineralization of **TP** by O_3 occur on a comparable timescale (Figure 5), a result most probably due to the relative high c_{O_3}, its relatively long lifetime and the larger reaction volume since ozonolysis takes place within the entire reactor volume. The results shown in Figure 4 confirm the earlier reported high rate of mineralization of the *ozonolysis* of **TP** [21], and in the absence of H_2O, oxidation by O_3 might contribute to the overall rate of mineralization of the VUV-

photochemical process. Under the given experimental conditions, O_3 oxidized **TP** ($c_{TP} \leq$ 18 ppm (v/v)) quantitatively but did not lead to complete mineralization. At higher c_{TP}, the major intermediate products of the oxidative degradation were separated and analyzed by GC/MS. The gas phase exiting the reactor contained primarily unreacted **TP** and **3**, their content depending on the initial c_{TP} (compounds drawn in red in Scheme 4). O_3 reacts by an electrophilic addition to the S-function of **TP** [58], and a dipolar intermediate (**17**, originally proposed to be the biradical generating a bicyclic primary ozonide [27]) might rearrange to yield **3** in eliminating O_2 (Scheme 4). A progressive oxidation of the S-function might compete with that reaction path. However, neither **15** nor **16** could be found, although the latter was generally assumed to be a stable product of **TP**-ozonolysis. Nevertheless, both pathways of reaction must finally lead to desulfurization (e.g. desulfoxidation) and oxidation of the remaining C_4-fragment (e.g. maleic dialdehyde (**18**)), to the formation of a number of low molecular weight alcohols, aldehydes and carboxylic acids and finally to CO_2.
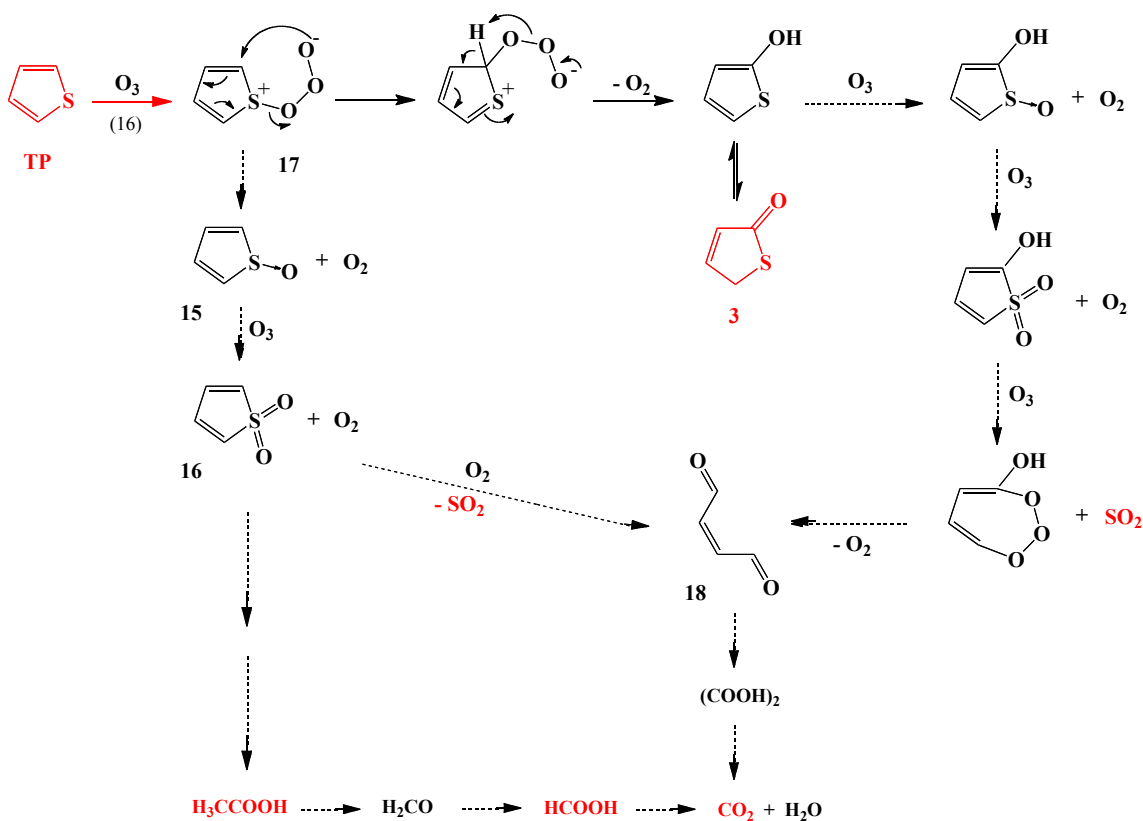
Scheme 4. Proposed pathways of reaction of the ozonolysis of thiophene (**TP**) to yield 5H-2-thiopheneone (**3**) and partial mineralization.

In addition to **TP** and **3**, 2-thiophene carboxaldehyde (**19**) and 2-formyl-2,3-dihydro-thiophene (**20**) were found in the exit gas of the ozonolysis ((compounds drawn in red in Scheme 5). Aldehydes are particularly interesting intermediate products, as they are needed to explain the presence of acylated **TP**-derivatives as well as compounds originating from subsequent reactions. **TP** is known to undergo condensation with carbonyl compounds, the corresponding reaction with formaldehyde (**21**) leading to 2-(hydroxymethyl)thiophene (**22**) that is oxidized to yield **19**. 2-Thiophene carboxylic acid (**23**) was not found as the compound might easily decarboxylate [59] to yield **TP**. A reductive step is needed for the production of **20** and might occur via 2,3-epoxy-thiophene (**24**). Acylation products indicate that upon introduction into the reactor, **TP** brought into or close to the irradiated volume was rapidly oxidized and degraded to desulfurized fragments containing carbonyl or carboxyl groups. These compounds are subsequently mixed with the substrate that remained outside of the irradiated volume and some of them may react within the time of residence or during sampling for analysis. During ozonolysis, a brown colored oil deposited in the annular reactor [60] which could be dissolved in acetonitrile for GC/MS-analysis. It contained, in addition to the oxidation products already mentioned, 2,2´-methylendithiophene (**25**), 3-(2-thienyl)-2-propenal (**26**) and diethylsulfone (**27**, compounds drawn in red in Schemes 5 and 6). The first may be obtained via acylation of **TP** with **19**; however, neither the resulting bis(2-thienyl) methanol (**28**) nor its oxidation product (bis(2-thienyl) ketone (**29**)) could be found. The reduction of **28** or **29** to **25** in the gas phase might be possible by redox reactions involving CO and H_2O with sulfides as promoters [e.g. 61]. 3-(2-thienyl)-2-propenal (**26**) is the acylation product of the reaction of malondialdehyde (**30**) with **TP**.
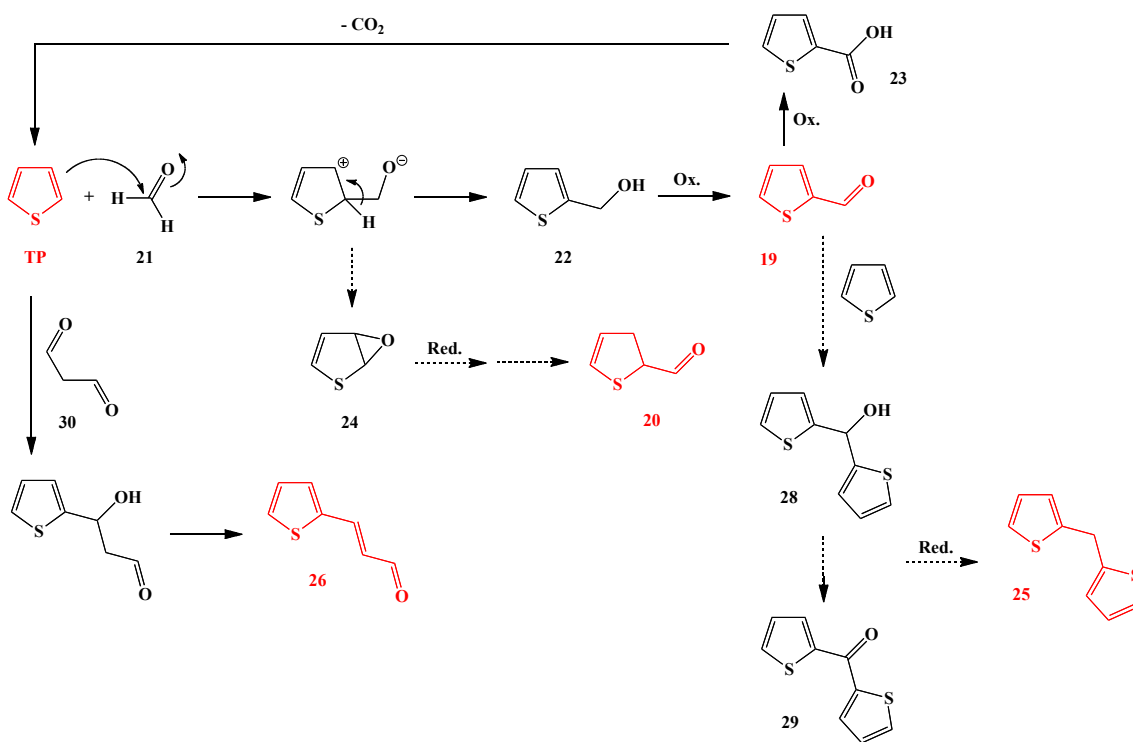
Scheme 5. Proposed pathways to yield products of aldehyde condensation during the oxidative degradation of thiophene (**TP**).

Ozonolysis of **TP** will also lead to **15** and subsequently to **16** (Scheme 4) [27]. A similar pathway of oxidation can also be drawn for **3** and other thiophene derivatives. However, no sulfoxides and, with the exception of diethylsulfone (**27**, Scheme 6), no sulfones could be identified and it may be assumed that the sulfoxides were oxidized instantaneously to the corresponding sulfones that reacted very fast *via* desulfoxidation to finally yield carbonyl and carboxyl compounds. There is no evident explanation for the formation of **27**.

The major intermediate products of oxidation found in the *VUV-photochemically initiated oxidative degradation* are the same as those found in the *ozonolysis* of **TP**.

In the presence of O_2, reaction (2) competes with the reaction of O with **TP**. In a first approximation, it might be assumed that the two reactions obey pseudo-first order kinetics. Under these conditions, the calculated rate $r_{O/O_2} = k_{O/O_2} c_{O_2} = 2.8 \times 10^{-12}$ cm^3 molecule^{-1} s^{-1} [21, 62] x 3.4 x 10^{22} molecule cm^{-3} is much higher than $r_{O/TP} = k_{O/TP} c_{TP} = 1.2 \times 10^{-11}$ cm^3 molecule^{-1} s^{-1} [34, 35] x 2 x 10^{18} molecule cm^{-3} and favors largely the

production of O_3. However, comparing the rates of the two pathways of **TP**-oxidation, the rate of oxidation by O_3 ($r_{O_3/TP} = k_{O_3/TP}\ c_{TP} = 6 \times 10^{-20}$ cm^3 molecule^{-1} s^{-1} x 2 x 10^{18} molecule cm^{-3}) is much smaller than the rate of the oxidation by O ($r_{O/TP} = k_{O/TP}\ c_{TP} = 1.2 \times 10^{-11}$ cm^3 molecule^{-1} s^{-1} x 2 x 10^{18} molecule cm^{-3}). Therefore, the contribution of O_3 to the overall rate of oxidation and oxidative degradation might not be prominent, even when a 10^4 times faster constant production of O_3 is taken into account. Since both reactions yield **3** as a relatively stable intermediate product of oxidation, the two pathways cannot be differentiated. As already shown in Schemes 1 and 4, reactions (5) to (7) and (16) (Scheme 4) lead to **3** as well as to **15**, and it may be assumed that these compounds represent the first intermediate products of the sequence of oxidative degradation.

Figure 4 shows that the rate of mineralization of the ozonolysis is about 30 to 40% compared to that of the VUV-photochemically initiated oxidative degradation. Since O_3 is not known to react with low-molecular weight carbonyl or carboxyl compounds, the higher rate of mineralization could be assigned to the high reactivity of O.

Beside the products of oxidation already mentioned, the presence of furan derivatives (2,5-furandione (maleic anhydride, **31**), 5H-2-furanone (4-Hydroxy-2-butenoic acid γ-lactone, **32**)) could be definitively established in the exit gas of the *VUV-photochemically initiated process in the presence of water vapor*. Maleic anhydride (**31**) might be formed from maleic acid in the hot gas phase (80 to 220ºC) passing the process and analytical equipments. The latter is thought to be produced by the oxidation of maleic dialdehyde (**18**) by HO˙ in the presence of H_2O. In a similar way, 5H-2-furanone (**31**) is most probably produced from 4-hydroxy-2-butenoic acid (**33**) that in turn is the product of an intramolecular Cannizzaro reaction of **18**. Dialdehydes are thought to be also typical products of desulfoxidation and subsequent addition of O_2 to the radical intermediates.
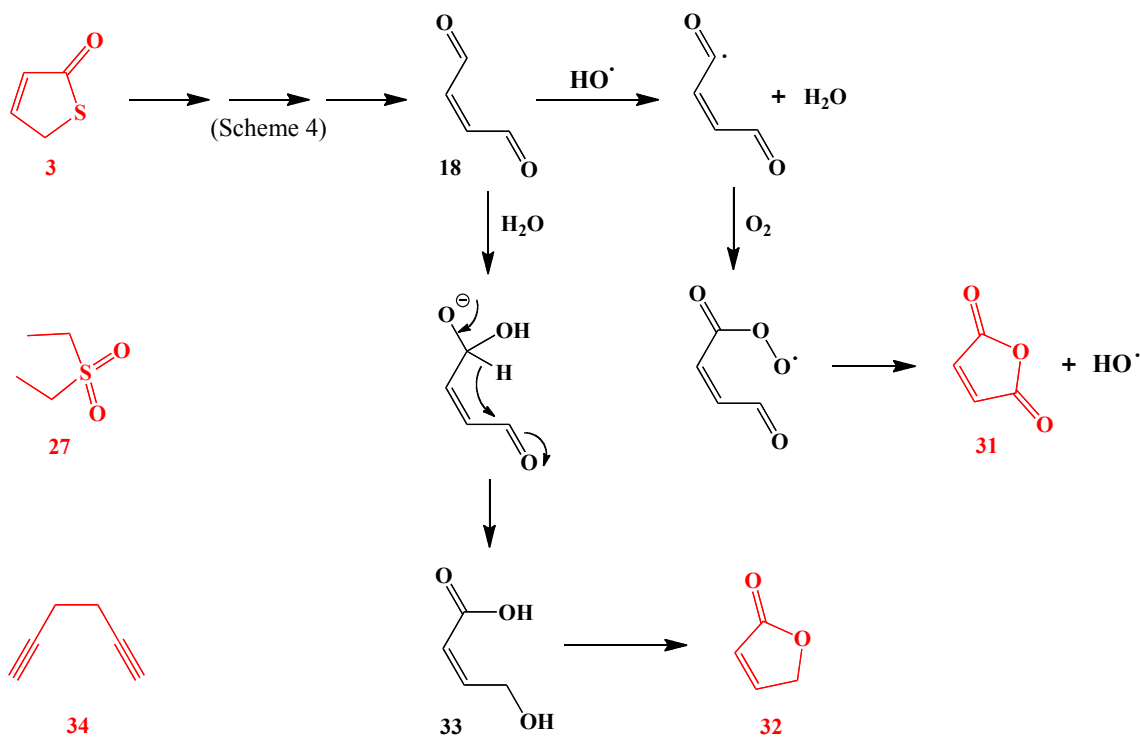
Scheme 6. Proposed pathways do yield furan derivatives during the VUV-photochemically initiated oxidative degradation of thiophene (**TP**).

The *VUV-photolysis of gaseous* **TP** *in the absence of molecular oxygen and H₂O* (nitrogen atmosphere) yielded carbon disulfide (CS_2), benzene, propyne (**14**), 1,5-hexadiyne (**34**, Scheme 6) and butadiene as major products. The result is in accord with the findings already published (Scheme 2), the C_6-compounds being due to combinations of radical intermediates. Small concentrations of benzene found in the presence of molecular oxygen indicate that the VUV-photolysis of **TP** was also taking place under experimental conditions of a photochemically initiated oxidation, where the primary intermediate radicals are trapped by O_2.

4. Conclusion

Total elimination of thiophene (**TP**) from the gas phase could be achieved by a VUV-photochemically initiated oxidation. The continuous process of **TP**-oxidation was

successful for substrate concentrations of up to 200 ppm (v/v). Under the same experimental conditions, total mineralization was found for **TP**-concentrations of less than 22 ppm (v/v). This is most probably due to the high values of absorbance at 172 nm of O_2, **TP** and H_2O and a too large optical path length of the annular photochemical reactor chosen resulting in large ratio of reactor to irradiated volumes. Under these conditions, "short circuiting" (s. ESI, *2.1.3. Evaluation of photolysis conditions*) is favored and cannot be compensated by the oxidation of **TP** with O_3 that is thought to diffuse over the whole reactor volume due to its longer lifetime. Addition of H_2O did not enhance the rate of neither oxidation nor mineralization.

The main intermediate products of the reaction network of oxidative degradation included 5H-2-thiopheneone (**3**), 2-thiophene carboxaldehyde (**19**), 2-formyl-2,3-dihydro-thiophene (**20**) and 3-(2-thienyl)-2-propenal (**26**). These products were formed by ozonolysis as well, and their production can be explained by the different pathways of oxidation initiated by O, O_3 and $HO^•$, respectively. In addition, furan derivatives (2,5-furandione (**31**) and 5H-2-furanone (**32**)) were identified in VUV-photochemical processes in the presence of water vapor. Proposals for the sequences of reactions leading to these products have been presented. For 2,2´-methylendithiophene (**25**) and diethylsulfone (**27**), steps of reduction would be required that cannot be explained by the results obtained.

The absence of sulfoxides and sulfones in the exit gas and kinetic data based on the results of SO_2-analyses indicate that the oxidation pathway via desulfurization (*e.g.* desulfoxidation) is as important as oxidation initiation by electrophilic addition or C-H-bond insertion in the 2-position of **TP**.

The results of this work indicate that the VUV-photochemically initiated oxidation is a technically valid process for the removal of **TP**. However, absorbance data require very small optical path lengths to achieve high efficiencies of mineralization. Under these conditions, the treatment of large fluxes of contaminated air needs multi-reactor installations that may not be economically feasible. Changing the length or height of a photochemical reactor finds its limits in the availability of VUV-radiation sources. Incomplete mineralization might lead to an exposure to products of oxidation that might be equally or even more toxic than the substrate. A VUV-photocatalyzed process might

have the potential to resolve this problem due to the combination of the photocatalyzed oxidation and the extended time of exposure of the adsorbed organic compounds to the highly reactive gaseous oxidants.

References

[1] F. Luck, Wet air oxidation: past, present and future, *Catal. Today*, 1999, **53**, 81 – 91.

[2] A. L. Linsebigler, G. Lu, J. T. Yates, Jr., Photocatalysis on TiO_2 Surfaces: Principles, Mechanisms, and Selected Results, *Chem. Revs.*, 1995, **95**, 735 - 758.

[3] M. Schwell, H.-W. Jochims, H. Baumgärtel, F. Dulieu, S. Leach, VUV photochemistry of small biomolecules, Planet. Space Sci., 2006, **54**, 1073 – 1085.

[4] J. Jeong, K. Sekiguchi, K. Sakamoto, Photochemical and photocatalytic degradation of gaseous toluene using short wavelength UV irradiation with TiO_2 catalyst: comparison of three UV sources, *Chemosphere*, 2004, **57**, 663 – 671.

[5] P. Zhang, J. Liu, Z. Zhang, VUV photocatalytic degradation of toluene in the gas phase, *Chem. Lett.*, 2004, **33**, 1242 - 1243.

[6] J. Jeong, K. Sekiguchi, W. Lee, K. Sakamoto, Photodegradation of gaseous volatile organic compounds (VOCs) using TiO_2 photoirradiated by an ozone-producing UV lamp: decomposition characteristics, identification of by-products and water-soluble organic intermediates, *J. Photochem. Photobiol. A: Chem.*, 2005, **169**, 279 – 287.

[7]   J. Jeong, K. Sekiguchi, M. Saito, Y. Lee, Y. Kim, K. Sakamoto, Removal of gaseous pollutants with a UV-C$_{254+185nm}$/TiO$_2$ irradiation system coupled with an air washer, *Chem. Eng. J.*, 2006, **118**, 127 – 130.

[8]   N. Quici, M. L. Vera, H. Choi, G. Li Puma, D. D. Dionysiou, M. I. Litter, H. Destaillats, Effect of key parameters on the photocatalytic oxidation of toluene at low concentrations in air under 254+185nm UV irradiation, *Appl. Catal. B*, 2010, **95**, 312 – 319.

[9]   H. Huang, D. Leung, Vacuum-ultraviolet photocatalysis: advanced process for toluene abatement, *J. Environ. Eng.*, 2011, **137**, 996 - 1001.

[10] P. Fu, P. Zhang, J. Li, Simultaneous elimination of formaldehyde and ozone byproduct using noble metal modified TiO$_2$ films in the gaseous VUV photocatalysis, *Int. J. Photoenergy*, 2012, 1 - 8.

[11] G. A. Loraine, W. H. Glaze, Destruction of Vapor Phase Halogenated Methanes by Means of Ultraviolet Photolysis. 47th Purdue Industrial Waste Conference Proceedings. Lewis Publishers, Chelsea MI, USA, 1992, 367 - 376.

[12] I. Gassiot, C. Baus, K. Schaber, A. M. Braun, VUV gas-phase photooxidation: a new tool for the degradation of VOCs in air, *J. Inf. Rec.*, 1998, **24**, 129 - 132.

[13] F. Fehti, J. López Gejo, M. Köhler, A. M. Braun, Vacuum-UV (VUV) photochemically initiated oxidation of dimethylamine in the gas phase, *J. Adv. Oxid. Technol.*, 2008, **11**, 208 - .

[14] C. Baus, K. Schaber, I. Gassiot Pintori, A. M. Braun, Separation and oxidative degradation of organic pollutants in aqueous systems by pervaporation and vaccuum-ultraviolet photolysis, *Sep. Purif. Technol.*, 2002, **28**, 125 - 140.

[15] M. Köhler, Untersuchungen VUV-photochemischer Prozesse in der Abgasbe-handlung und zur Oberflächenfunktionalisierung bei Membranprozessen, PhD thesis, Universität Karlsruhe, Germany, 2006

[16] J. Salas Vicente, J. López Gejo, S. Rothenbacher, Sumalekshmy Sarojiniamma, E. Gogritchiani, M. Wörner, G. Kasper, A. M. Braun, Oxidation of polystyrene aerosols by vuv-photolysis and/or ozone, *Photochem. Photobiol. Sci.*, 2009, **8**, 944 - 953.

[17] K. G. Kropp, P. M. Fedorak, A review of the occurrence, toxicity and biodegradation of condensed thiophenes found in petroleum, *Can. J. Microbiol.*, 1998, **45**, 605 – 622.

[18] D. K. Dalvie, A. S. Kalgutkar, S. C. Khojasteh-Bakht, R. S. Obach, J. P. O´Donnell, Biotransformation reactions of five-membered aromatic heterocyclic rings, *Chem. Res. Toxicol.* 2002, **15**, 269 - 299.

[19] J. Swanston, Thiophene, in Ullmann's Encyclopedia of Industrial Chemistry, 6th edition, Wiley-VCH, Weinheim, 2006, vol. 40.

[20] J. G. Calvert, J. N. Pitts Jr., *Photochemistry,* John Wiley & Sons, New York 1966.

[21] B. A. Kaduk, S. Toby, The reaction of ozone with thiophene in the gas phase , *Int. J. Chem. Kinet.* 1977, **9**, 829 - 840.

[22] a) R. Atkinson, S. M. Aschmann, W. P. L. Carter, Kinetics of the Reactions of O_3 and OH Radicals with Furan and Thiophene at 298 +/- 2 K, *Int. J. Chem. Kinet.* 1983, **15**, 51 - 61.
b) R. Atkinson, W.P. Carter, Kinetics and mechanisms of the gas-phase reactions of ozone with organic compounds under atmospheric conditions, *Chem. Rev.*, 1984, **84**, 437 - 470.

[23] H. Macleod, J. L. Jourdain, G. Le Bras, Absolute rate constant for the reaction of OH with thiophene between 293 and 473 K, *Chem. Phys. Lett.,* 1983, **98**, 381 - 285.

[24] P. H. Wine, R. J. Thompsom, Kinetics of OH reactions with furan, thiophene, and tetrahydrothiophene, *Int. J. Chem. Kinet.,* 1984, **16**, 867 - 878.

[25] D. Martin, J. L. Jourdain, G. Le Bras, Kinetic study for the reactions of OH radicals with dimethylsulfide, diethylsulfide, tetrahydrothiophene, and thiophene, *Int. J. Chem. Kinet.,* 1985, **17**, 1247 - 1261.

[26] a) T. J. Wallington, Kinetics of the gas phase reaction of OH radicals with pyrrole and thiophene, *Int. J. Chem. Kinet.*, 1985, **18**, 487 - 496.
b) J. H. Lee, I. N. Tang, Absolute rate constants for the hydroxyl radical reactions with ethane, furan, and thiophene at room temperature, *J. Chem. Phys.,* 1982, **77**, 4459 - 4463.

[27] H. A. Wiebe, J. Heicklen, Photolysis of thiophene vapor, *Can. J. Chem.* 1969, **47**, 2965 - 2979.

[28] S. Nourbakhsh, K. Norwood, H.-M. Yin, C.-L. Liao, C. Y. Ng, Vacuum ultraviolet photodissociation and photoionization studies of CH_3SCH_3 and CH_3S, *J. Chem. Phys.*, 1991, **95**, 5014 - 5023.

[29] T. A. A. Oliver, G. A. King , M. G. D. Nix, M. N. R. Ashfold, Ultraviolet Photodissociation Dynamics of 2-Methyl, 3-Furanthiol: Tuning π-Conjugation in Sulfur Substituted Heterocycles, *J. Phys. Chem. A*, 2010, **114**, 1338 – 1346.

[30] C.-W. Hsu, C.-L. Liao, Z.-X. Ma, C. Y. Ng, Direct Identification of Photofragment Structures Formed in the 193 nm Photodissociation of Thiophene, *J. Phys. Chem.,* 1995, **99**, 1760 - 1767.

[31] S. Hatakeyama, M. Okuda, H. Akimoto, Formation of sulfur dioxide and methanesulfonic acid in the photooxidation of dimethyl sulfide in the air, *Geophys. Res. Lett.*, 1982, 583 - 586.

[32] T. M.Hashem, M. Zirlewagen, A. M. Braun, Simultaneous photochemical generation of ozone in the gas phase and photolysis of aqueous reactions systems using one vuv light source, *Water Sci. Techn.*, 1997, **35**, 41 - 48.

[33] C. Geletneky, S. Berger, The Mechanism of Ozonolysis Revisited by ^{17}O-NMR Spectroscopy, *Eur. J. Org. Chem.*, 1998, 1625 – 1627.

[34] J. H. Lee, I. N. Tang, Absolute rate constant for the reaction of $O(^3P)$ with thiophene from 238 to 448 K, *J. Chem. Phys.*, 1981, **75**, 137 - 140.

[35] X. Gao, M. P. Hall, D. J. Smith, R. Grice, Dynamics of Ring Cleavage and Substitution in the Reactive Scattering of $O(^3P)$ Atoms with C_2H_4S and C_4H_4S Molecules, *J. Phys. Chem. A*, 1997, **101**, 187 - 191.

[36] C. Barckholtz, T. A. Barckholtz, C. M. Hadad, A Mechanistic Study of the Reactions of H, O (^3P), and OH with Monocyclic Aromatic Hydrocarbons by Density Functional Theory, *J. Phys. Chem. A*, 2001, **105**, 140 - 152.

[37] M. J. Heying, M. Nag, W. S. Jenks, Photochemistry of thiophene-*S*-oxide derivatives, *J. Phys. Org. Chem.*, 2008, **21**, 915 - 924.

[38] T. Thiemann, D. J. Walton, A. Oliveira Brett, J. Iniesta, F. Marken, Y. Li, The chemistry of thiophene *S*-oxides and related compounds, *Arkivoc*, 2009, 96 - 113.

[39] M. C. Gonzalez, E. Oliveros, M. Wörner, A. M. Braun, Vacuum-ultraviolet photolysis of aqueous reactions systems, *Photochem. Photobiol. C: Rev.*, 2004, **5**, 225 - 246.

[40] O. Legrini, E. Oliveros, A. M. Braun, Photochemical Processes for Water Treatment, *Chem. Rev.*, 1993, **93**, 671 - 698.

[41] B. B. Saunders, P. C. Kaufman, M. S. Matheson, Reactions of thiophene with radiolytically produced radicals, Part I, the hydroxyl radical, *J. Phys. Chem.*, 1978, **82**, 142 – 150.

[42] M. H. Palmer, I. C. Walker, M. F. Guest, The electronic states of thiophene studied by optical (VUV) absorption, near-threshold electron energy-loss (EEL) spectroscopy and ab initio multi-reference configuration interaction calculations, *Chem. Phys.*, 1999, **241**, 275 - 296.

[43] J. Wan, M. Hada, M. Ehara, H. Nakatsuji, Electronic Excitation Spectra of Thiophene Studied by Symmetry-Adapted Cluster Configuration Interaction Method, *J. Chem. Phys.*, 2001, **114**, 842 - 850.

[44] M. Bajic, K. Humski, L. Klasinc, B. Ruscic, Substitution effects on electronic structure of thiophene, *Z. Naturforsch. B*, 1985, **40**, 1214 - 1218.

[45] W. C. Price, A. D. Walsh, The Absorption Spectra of the Cyclic Dienes in the Vaccum Ultra-Violet, *Proc. Roy. Soc. A.*, 1941, **179**, 201 - 214.

[46] A. K. Nayak, S. K. Sarkar, R. S. Karve, V. Parthasarathy, K. V. S. Rama Rao, J. P. Mittal, S. L. N. G. Krishnamachari, T. V. Venkitachalam, Infrared laser multiple photon dissociation of thiophene in gas phase, *Applied Physics B*, 1989, **48**, 437 – 443.

[47] S. L. N. G. Krishnamachari, T. V. Venkitachalam, A new transient absorption spectrum observed in the flash photolysis of thiophene, *Chem. Phys. Lett.*, 1978, **55**, 116 - 118.

[48] J. D. Myers, PhD Thesis, University of California, 1993, cited in [49].

[49] F. Qi, O. Sorkhabi, A. H. Rizvi, A. G. Suits, 193 nm photodissociation of thiophene probed using synchrotron radiation, *J. Phys. Chem. A* 1999, **103**, 8351 - 8358.

[50] F. Benoit-Marquié, M. T. Boisdon, A. M. Braun, E. Oliveros, M. T. Maurette, Dégradation de composés organiques en phase gazeuse par photocatalyse et par photolyse V-UV - Organic compound degradation in gas phase by photocatalysis and by V-UV photolysis, *Entropie,* 2000, **228**, 36 - 43.

[51] R. Zellner, G. Wagner, B. Himme, H_2 Formation in the Reaction of O (^{1}D) with H_2O, *J. Phys, Chem*., 1980, **84**, 3196 - 3198.

[52] S. Matsuzawa, J. Tanaka, S. Satoa, T. Ibusukia, Photocatalytic oxidation of dibenzothiophenes in acetonitrile using TiO_2: effect of hydrogen peroxide and ultrasound irradiation, *J. Photochem. Photobiol. A: Chemistry*, 2002, **149**, 183 - 189.

[53] M.C. Canela, R.M. Alberici, C.R. Sofia, M.N. Eberlin, W.F. Jardim, Destruction of Malodorous Compounds Using Heterogeneous Photocatalysis, *Environ. Sci. & Technol.*, 1999, **33**, 2788 - 2792.

[54] A. Maggiolo, E. A. Blair, Ozone Oxidation Of Sulfides And Sulfoxides, *Adv. Chem*., 1969, **21**, Chapt. 30, 200 - 201.

[55] G. Heit, A. Neuner, P.-Y. Saugy, A. M. Braun, Vacuum-UV (172 nm) Actinometry. The Quantumyield of the Photolysis of Water, *J. Phys. Chem*., 1998, **102**, 5551 - 5561.

[56] G. Heit, A.M. Braun, VUV Photolysis of Aqueous Systems: Spatial Differentiation between Volumes of Primary And Secondary Reactions, *Water Sci.Techn*., 1997, **35**, 25 - 30.

[57] R. Atkinson, Kinetics and Mechanisms of the Gas-Phase Reactions of the Hydroxyl Radical with Organic Compounds, *J. Phys. Chem. Ref. Data*, Monograph No. 1 (1989).

[58] Q. E. Thompson, Ozone Oxidation of Nucleophilic Substances. I. Tertiary Phosphite Esters, *J. Am. Chem. Soc.*, 1961, **83**, 845 – 851.

[59] N. Quici, M.I. Litter, A.M. Braun, E. Oliveros, Vacuum-uv photolysis of aqueous solutions of citric and gallic acid, *J. Photochem. Photobiol. A: Chemistry*, 2008, **197**, 306-312.

[60] P. K. Arora, J. P. S. Chatha, Chemiluminescence from the reactions of ozone with sulphur compounds, *Can. J. Chem*., 1984, **62**, 417 - 423.

[61] V. I. Stenberg, D. Wettlaufer, R. J. Baltisberger, C. L. Knudson, N. F. Woolsey, Benzophenone reduction using sulphur-based additives, *Fuel*, 1983, **62**, 1324 - 1235.

[62] C. L. Lin, M. T. Leu, Temperature and third-body dependence of the rate constant for the reaction $O + O_2 + M \longrightarrow O_3 + M$, *Intl J. Chem. Kin.*, 1982, **14**, 417 - 434.